Chalcogenide Letters Vol. 18, No. 4, April 2021, p. 171 - 181

Alteration on the chemical durability of tellurite glass: effect of heat treatment

S. F. Yuhari[a], A. Awang[a,*], M. A. A. Rajak[b], J. Dayou[c]
[a]*Physics with Electronics Programme, Faculty of Science and Natural Resources, Universiti Malaysia Sabah, 88400 Kota Kinabalu, Sabah, Malaysia*
[b]*Preparatory Centre for Science and Technology, Universiti Malaysia Sabah, 88400 Kota Kinabalu, Sabah, Malaysia*
[c]*Energy, Vibration and Sound Research Group (e-VIBS), Faculty of Science and Natural Resources, Universiti Malaysia Sabah, 88400 Kota Kinabalu, Sabah, Malaysia*

Modifying the glass features under controlled parameters is vital to achieving optimum final product for diverse applications. In this study, tellurite glass was prepared using melt quenching technique and heat treated at varying temperatures. The thermal stability, chemical durability, and surface morphology were investigated by implementing DTA and SEM-EDX. TZNE glass possesses ΔT of 115 °C. The weight loss of glass in distilled water and ammonium hydroxide solution became apparent for glass heat treated at higher temperature due to decrease in its structural stability. SEM micrographs manifested the emergence of acicular shape and globular shape particles deposited on the glass surface.

(Received February 6, 2021; Accepted April 6, 2021)

Keywords: Heat treatment, Thermal stability, Non-bridging oxygen, Chemical durability, Corrosion

1. Introduction

Glass has been acknowledged as corrosion-proof since glass is very resistant to corrosion. This feature makes glass unique in comparison to other materials. Though, glass is chemically attacked when it is exposed to certain conditions [1]. Chemical durability of glass signifies its resistance to the attack of aqueous solutions and atmospheric agents [2]. However, the chemical composition of glass and the nature of aqueous solution affect the chemical durability of glass in different media. Moreover, chemical durability depends on the bond strength, field strength, and volume of various cations present in the glass [3]. Tellurite glass has been proved to be more effective in a wide range of applications compared to silicate, phosphate, and borate-based glass due to its beneficial features of good thermal stability, chemical durability, and rare earth (RE) solubility. Great thermal stability of tellurite glass makes it tolerable and helps it to function at high temperature ranges and also to emerge as a good solid-state material [4–6].

TeO_2 is categorized as an expensive rarely-found element in the earth's crust, which are two shortcomings of tellurite glass [7]. A huge attempt has been made to manipulate the composition of glass systems, for example, by incorporation of different modifiers and nanoparticles to achieve optimum chemical durability [8–10]. The introduction of simple binary or ternary systems by incorporation of additive materials in tellurite host glass has opened a new path [7]. Nonetheless, in-depth insight into the thermal and chemical durability of glass is vital to aforementioned applications. In the present study, tellurite glass is synthesized using the melt quenching technique with a distinctive range of heat treatment temperature. The thermal properties, chemical durability, and surface morphology of glass are characterized with the implementation of DTA and SEM-EDX. The effects of heat treatment on the modification of the thermal properties, chemical durability, and surface morphology of glass are addressed further.

* Corresponding author: asmahani_awang@yahoo.com
https://doi.org/10.15251/CL.2021.184.171

2. Experimental details

The glass composition of $70TeO_2–20ZnO–9.5Na_2O–0.5Er_2O_3$ in mol% were synthesized using the melt-quenching technique. The specific weights of TeO_2, ZnO, Na_2O, and Er_2O_3 powders were mixed thoroughly. The batches were subjected to a milling process for 30 minutes to obtain a homogenous mixture. A platinum crucible containing glass constituents were placed in a furnace with temperature of 970 °C for 30 minutes. Then, the molten was poured in a brass mould and annealed for 3 hours at 300 °C before cooling down to room temperature. Afterward, the prepared glass was subjected to heat treatment with annealing temperature varied from 325 °C, 350 °C, 375 °C and 400 °C for 2 hours and then subjected to cooling-down process to room temperature. The transparent glass samples were cut and polished for further characterization. The glass code and glass composition with varying heat treatment temperature are tabulated in Table 1.

Table 1. Glass composition with varying heat treatment temperature (HT).

Glass code	TeO_2	ZnO	Na_2O	Er_2O_3	HT (°C)
TZNE	70	20	9.5	0.5	-
TZNE-HT325	70	20	9.5	0.5	325
TZNE-HT350	70	20	9.5	0.5	350
TZNE-HT375	70	20	9.5	0.5	375
TZNE-HT400	70	20	9.5	0.5	400

The glass transition temperature (T_g), onset crystallization temperature (T_x) and crystallization temperature (T_C) were measured using the Differential Thermal Analysis (DTA) of Shimadzu DTG-60H. The glass formation ability or glass stability against crystallization was evaluated by the following relation [11,12]:

$$\Delta T = T_x - T_g \tag{1}$$

where ΔT is the glass stability.

To evaluate the chemical durability, the glass sample was weighed using analytical digital balance with error of ± 0.0001 gm. Then, the glass sample was immersed completely in different aqueous solutions for distilled water and ammonium hydroxide solution (Mallickrodt chemical, 30% NH_4OH). The sample was kept in a sealed bottle with duration of 10 days for distilled water and 3 days for ammonium hydroxide solution. After specific time duration was achieved, the glass sample was subjected to the drying process at room temperature and weighed using analytical balance. The experiment was performed in room temperature. The weight loss (W_L) was calculated using the following equation [8-10,13,14]:

$$W_L = \frac{W_B - W_A}{W_A} \times 100 \tag{2}$$

where W_A and W_B represent the weights of glass after and before immersion in aqueous solution.

The morphology of the glass surface was investigated using a TM3000 Hitachi tabletop scanning electron microscope (SEM) with a resolution of 20 micron.

3. Results and discussion

Determination of the thermal stability for non-heat-treated glass (TZNE glass) is important to identify the specific range of operating temperatures that stimulates the crystallization process in glass and implies resistance against crystallization of glass through the nucleation and growth process [15,16]. Figure 1 shows the DTA curves of glass sample without heat treatment (TZNE glass) in the range of 0–1000 °C. The glass transition temperature (T_g) in the TZNE glass was

located at 300 °C. The onset crystallization temperature (T_x) was evidenced at 415 °C. Meanwhile, two crystallization temperatures (T_{C1} and T_{C2}) were located at 435 °C and 696 °C, respectively. Two crystallization peaks manifested different crystallization mechanisms leading to the phase separation in the glass sample [16,17]. The TeO_2 crystallizing phase was represented by the appearance of crystallization peaks at lower temperature. Meanwhile, the Zn_3TeO_6 crystallization phase was represented by the emergence of crystallization peaks at higher temperature [18]. In the present study, the value of ΔT is 115 °C, which is higher than 100 °C, indicating that our glass possesses relatively good thermal stability [19]. The thermal parameter for TZNE glass is displayed in Table 2.

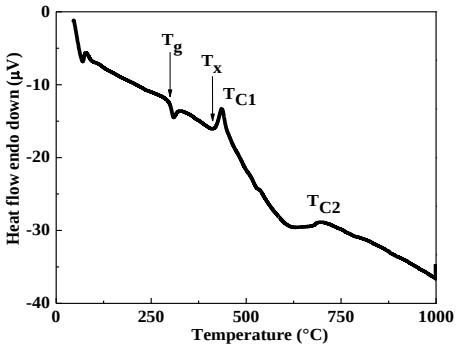

Fig. 1. DTA curve of TZNE glass.

Table 2. Thermal parameters of TZNE glass.

Glass code	T_g (°C)	T_x (°C)	T_{C1} (°C)	T_{C2} (°C)	ΔT (°C)
TZNE	300	415	435	696	115

An investigation was performed on the physical appearance and weight loss of glass for 3 days of immersion in distilled water. No significant change was observed in the physical appearance and the loss weight of glass. Therefore, the time duration to investigate the apparent changes on glass surface was increased to 10 days. The physical appearance of the glass surface after 10 days of immersion in distilled water is illustrated in Fig. 2. The color of the glass sample was evidenced to change from bright orange to pale orange. Meanwhile, Fig. 3 shows the physical appearance of glass samples after 3 days of immersion in ammonium hydroxide solution. The formation of white powder layers on the glass surface after a few hours of immersion are observed due to the interaction between glass and ammonium hydroxide solution. After 3 days of immersion in ammonium hydroxide solution, all glass samples were evidenced to turn opaque, completely covered by a white layer and the thickness of glass samples were depleted severely. In this stage, the glass samples were fragile and needed to be handled meticulously during the weight loss measurement.

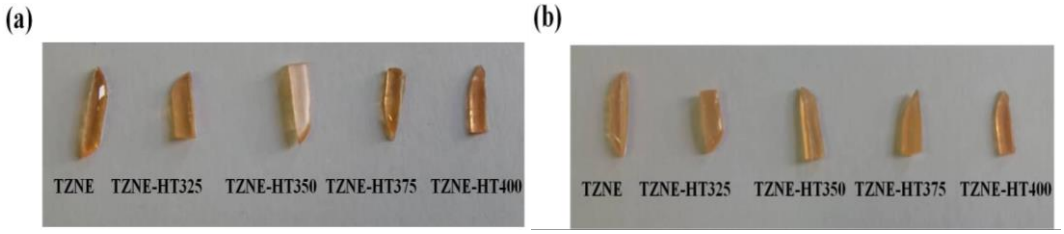

Fig. 2. Physical appearance of tellurite glass (a) before immersion in distilled water (b) after 10 days of immersion in distilled water.

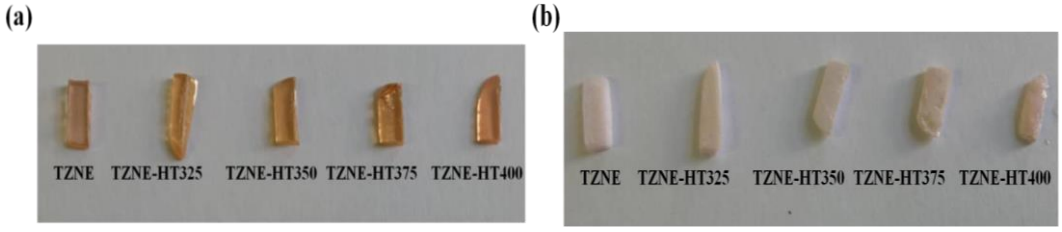

Fig. 3. Physical appearance of tellurite glass (a) before immersion in ammonium hydroxide solution (b) after 3 days of immersion in ammonium hydroxide solution.

Table 3 summarizes the weight loss of the glass samples in different immersion solutions. The weight loss of the samples after immersion in distilled water ranged from 3.88% to 40.26%. Meanwhile, the weight loss of the glass samples increased further when using ammonium hydroxide as an immersion solution; this time, the weight loss value ranged from 64.55% to 102.28%. Higher weight loss was observed in the glass samples when immersed in ammonium hydroxide as an immersion solution due to the strong alkaline nature of the solution. Figure 4 shows variations in the weight loss of the samples with different heat treatment temperatures immersed in distilled water and ammonium hydroxide solution. In this study, the highest weight loss beyond 100% implies the massive weight loss experienced by the TZNE-HT400 glass. The same pattern of the weight loss of glass beyond 100% was reported by Mahraz et al. [8]. Our results are in good agreement with those of a study previously conducted by Kim et al. [9] in which a significant increase was observed in the weight loss of heat-treated glass samples. The chemical composition, bond strength, bond lengths, and coordination number of the atom in a glass matrix affect the corrosion rate of glass [8]. In our study, heat treatment at 400 °C (approaching the T_x value) contributes to the nucleation process [12] stimulating the devitrification in glass [20]. Therefore, modification on the glass structure occurred during heat treatment [9,21,22] generates more non-bridging oxygen (NBO), which reduces the resistance of glass towards chemical attack [23]. Continuous exposure of glass to the aqueous solution of distilled water and ammonium hydroxide causes corrosion on the glass surface and leads to a significant weight loss [24].

Table 3. Glass code and variation in weight of the samples before and after immersion in distilled water and ammonium hydroxide solution.

Glass code	Weight loss in distilled water, $W_{L(water)}$ (%)	Weight loss in ammonium hydroxide, $W_{L(ammonium)}$ (%)
TZNE	3.88	64.55
TZNE-HT325	3.94	66.47
TZNE-HT350	11.35	68.04
TZNE-HT375	23.50	68.33
TZNE-HT400	40.26	102.28

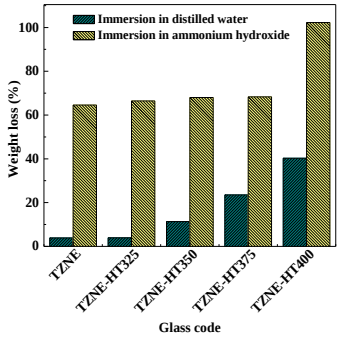

Fig. 4. Weight loss (%) of glass after immersion in different aqueous solutions.

SEM micrographs give information regarding the surface morphology of glass after immersion in the aqueous solution. Singh et al. [25] reported that the nature of glass affects the interaction between glass and different types of aqueous solutions. In another study conducted by Walters et al. [26], the corrosion process in the glass was observed to be associated with three stages of attack. The first step involves an ion exchange reaction leading to dissolution of one or more components of glass, hence leads to the formation of a spongy layer on the glass surface. In this process, the surface damage occurs due to the leaching attack by tarnishing or staining on the glass surface. The second mechanism known as etching illustrates the total dissolution of glass. The third step, which is known as the shiroyake process, leads to the deposition of the insoluble elements on the glass surface. In this study, we found that the heat treatment process generates more NBO in the glass network [27]. The NBO forms a weak bond connected to the glass network [28]. Therefore, higher concentration of NBO in the glass network facilitates the dissolution of glass in aqueous solution [10,23].

The corrosion of glass by distilled water can be divided into three chemical reactions [24,29]. The first step involves the replacement of alkali ion into solution due to the penetration of a proton from water into the glassy network:

$$\equiv \mathrm{Te} - \mathrm{OR} + \mathrm{H_2O} \rightarrow \equiv \mathrm{Te} - \mathrm{OH} + \mathrm{R^+} + \mathrm{OH^-} \quad (3)$$

In the second step, the hydroxyl ion in solution disrupts bonding in glass network by:

$$\equiv \mathrm{Te} - \mathrm{O} - \mathrm{Te} \equiv + \mathrm{OH^-} \rightarrow \equiv \mathrm{Te} - \mathrm{OH} + \equiv \mathrm{Te} - \mathrm{O^-} \quad (4)$$

Then, in the third step, a hydroxyl ion is produced due to the interaction of the NBO in Equation (4) with water molecules as follows:

$$\equiv \mathrm{Te} - \mathrm{O} + \mathrm{H_2O} \rightarrow \equiv \mathrm{Te} - \mathrm{OH} + \mathrm{OH^-} \quad (5)$$

Figure 5(a)–(e) shows the surface morphologies of the glass samples heat treated at varying temperatures after 10 days of immersion in distilled water. The SEM image illustrates the appearance of wide acicular shape particles. The acicular shape particles accumulated and formed the flower-like shaped particles [8]. The deposition and accumulation of products on the glass surface within a longer time interval implies a slower attack in more resistant glasses. The process is repeated and the glass is continuously attacked once the glass is exposed to the aqueous medium. This process leads to a gradual dissolution of glass [1].

The corrosion of the glass sample by ammonium hydroxide solution can be described using the following equation [13,14]:

$$\equiv \mathrm{Te} - \mathrm{O} - \mathrm{Te} \equiv + \mathrm{OH^-} \rightarrow \equiv \mathrm{Te} - \mathrm{OH} + \equiv \mathrm{Te} - \mathrm{O} \quad (6)$$

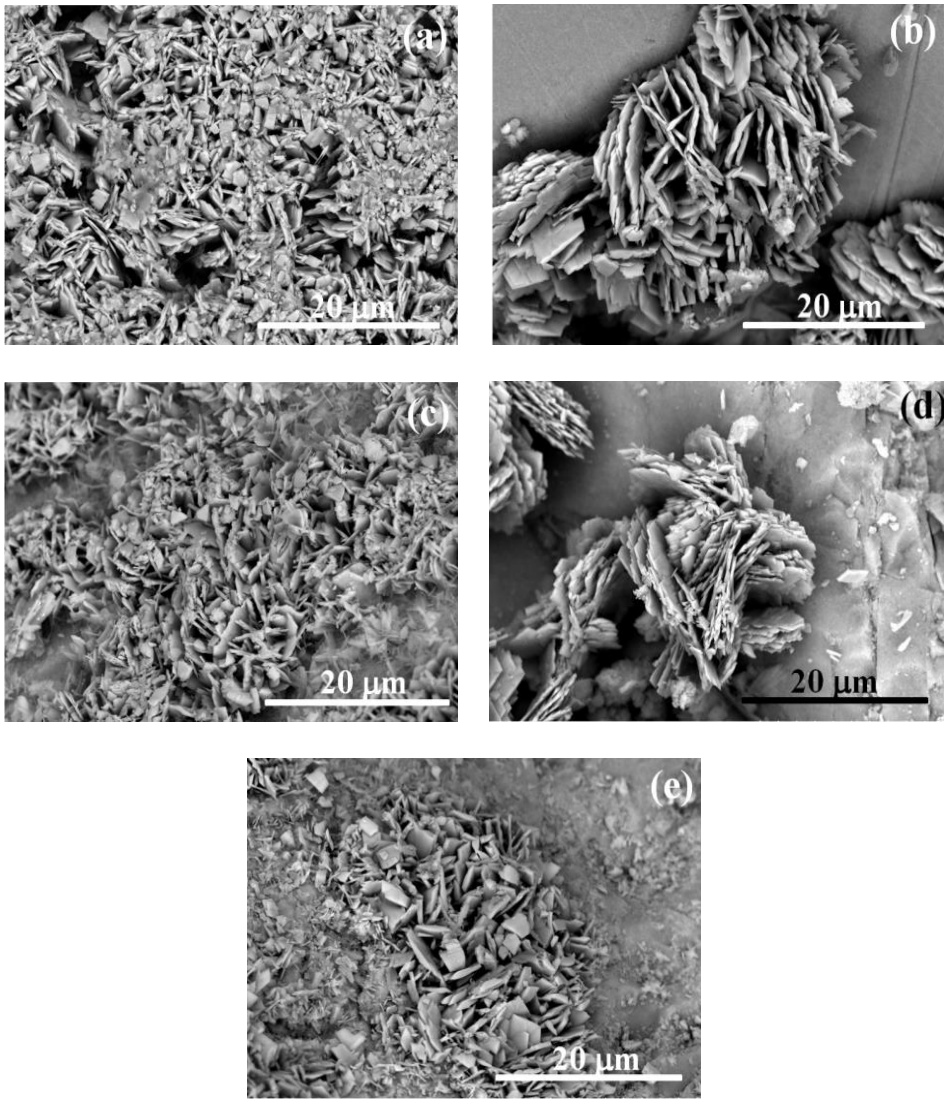

Fig. 5. SEM micrographs of the glass samples after 10 days of immersion in distilled water for (a) TZNE glass (b) TZNE-HT325 glass (c) TZNE-HT350 glass (d) TZNE-HT375 glass and (e) TZNE-HT400 glass.

The glass dissolution process in alkaline solution can be divided into a few elementary steps. In the first step, the diffusion of hydroxide ions through the bulk solution phase occurred. The second step involves the hydroxide ions in contact with the localized glass surface and subsequently triggered potential reaction. The glass dissolution occurred due to the interaction of the hydroxide ions with the glass surface [13]. Figure 6(a)–(e) shows the surface morphologies of glass samples under varying heat treatment temperature after 3 days of immersion in ammonium hydroxide solution. By comparing the SEM images presented in Fig. 5 and 6, it is found that the immersion of the glass samples in different aqueous solutions displayed the transformation in the grain shape, size, and the surface state of glass. In fact, different mechanisms occurred on the glass surface by using different aqueous solutions as immersion liquid. The formation of thick layers which are detached by fragments leads to unprotected glass signifies a quick attack in less resistant glasses towards an alkaline environment [1]. Furthermore, the SEM image illustrates the appearance of surface fracture as evidenced in Fig. 6(a)–(d). According to Papadopoulos and Drosou [1], fragments of the network vanish and glass structures are strongly affected in an alkaline environment. In this condition, the hydroxyl ions attack the glass framework when the glass is in contact with alkaline solution. Figure 6(e) illustrates the appearance of globular shape and acicular shape particles deposited on the glass surface due to the phase separation [20]. The

formation of globular was observed due to the nucleation of glass at higher heat treatment temperature at 400 ℃ and reacting with ammonium hydroxide solution. The formation of acicular shape particles was evidenced due to the rich-tellurium glass area reacting with ammonium hydroxide solution [14].

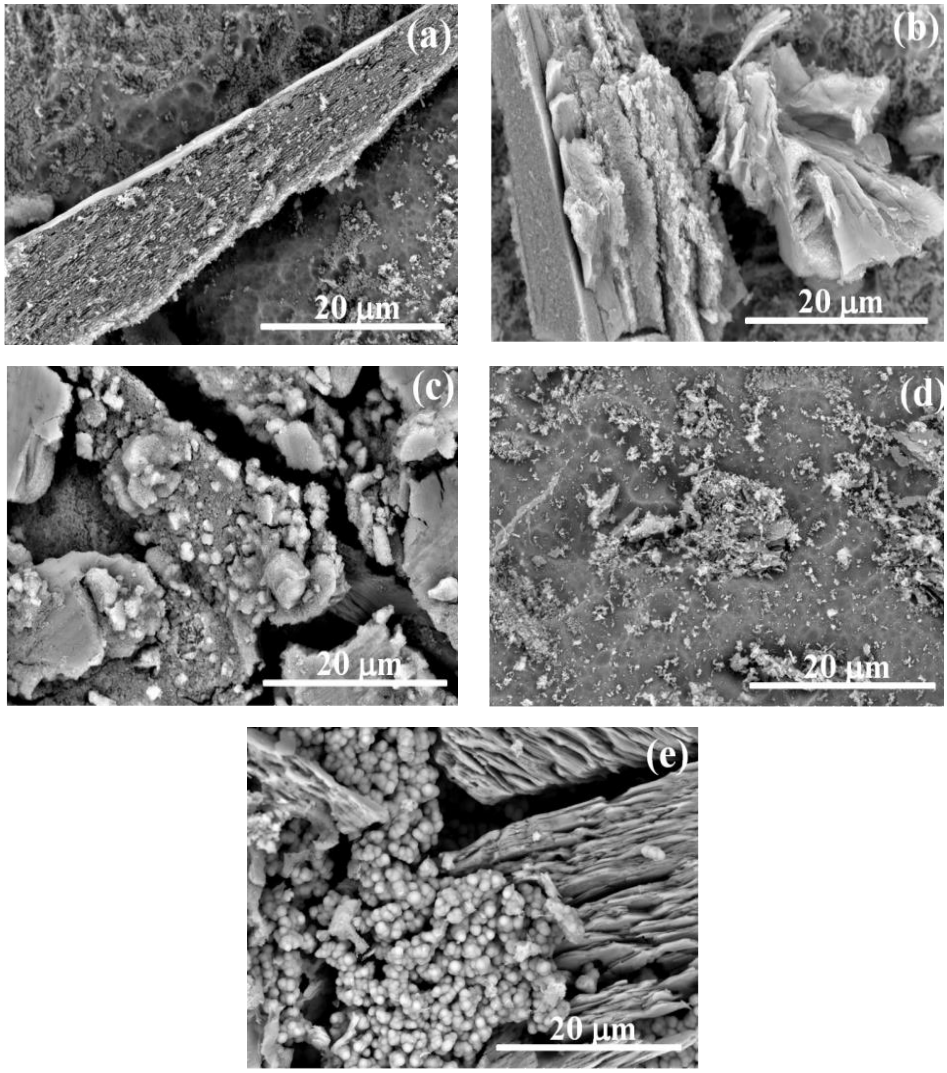

Fig. 6. SEM micrographs of the glass samples after 3 days of immersion in ammonium hydroxide solution for (a) TZNE glass (b) TZNE-HT325 glass (c) TZNE-HT350 glass (d) TZNE-HT375 glass and (e) TZNE-HT400 glass.

The current glass composition experienced slower attack by using distilled water as immersion solution and indicates the glass more resistant to distilled water. However, glass shows a quick attack in alkaline environment and signifies the less resistant features of glass towards alkaline environment. Figure 7 and 8 shows the EDX spectra of corroded glass by using distilled water and ammonium hydroxide as immersion solution. The EDX spectra from a selected spot from the SEM image display the existence of carbon (C), oxygen (O), zinc (Zn), tellurium (Te) and gold (Au). The appearance of Au peak is evidenced due to the coating materials. The application of a conducting surface coating on the glass surface provides a path for the incident electrons to flow to ground due to the glass possesses non-conducting properties [30].

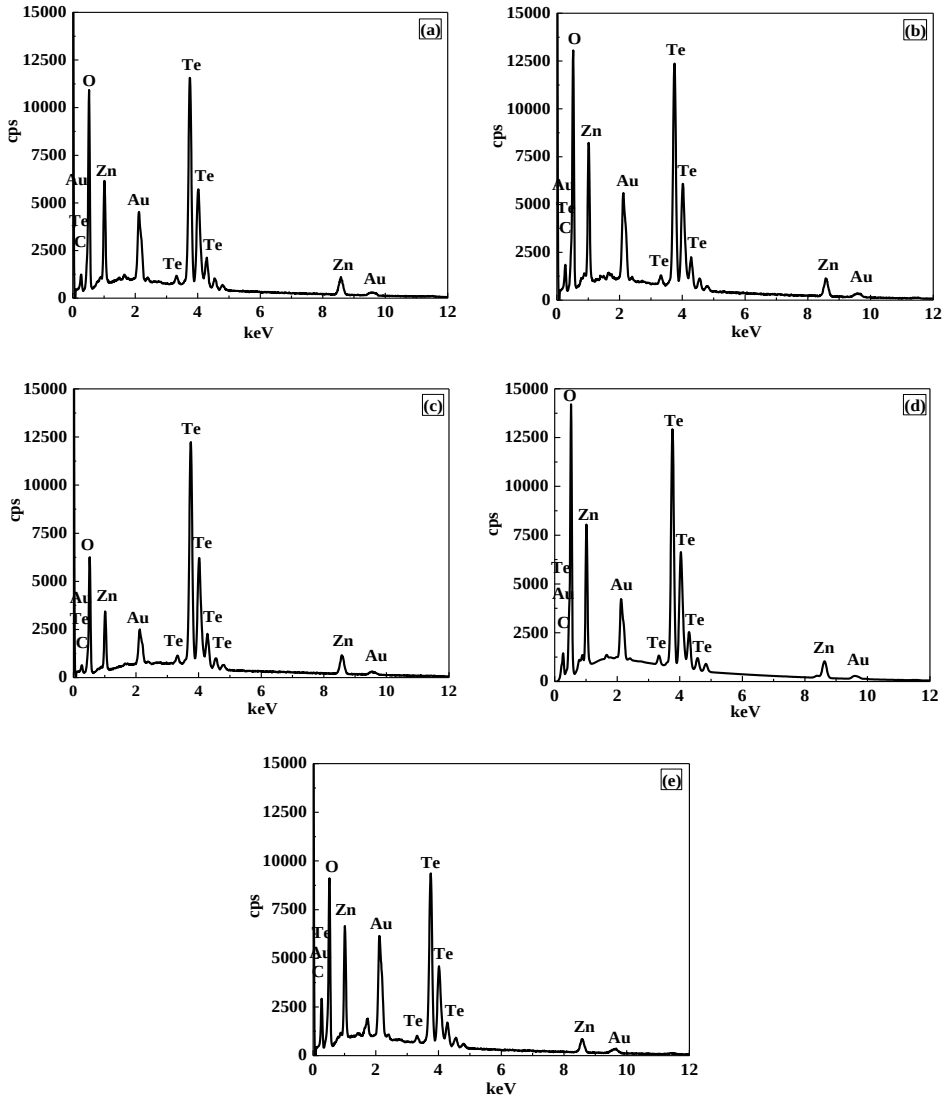

Fig. 7. EDX spectra of corroded glass with distilled water as immersion solution for (a) TZNE glass (b) TZNE-HT325 glass (c) TZNE-HT350 glass (d) TZNE-HT375 glass and (e) TZNE-HT400 glass.

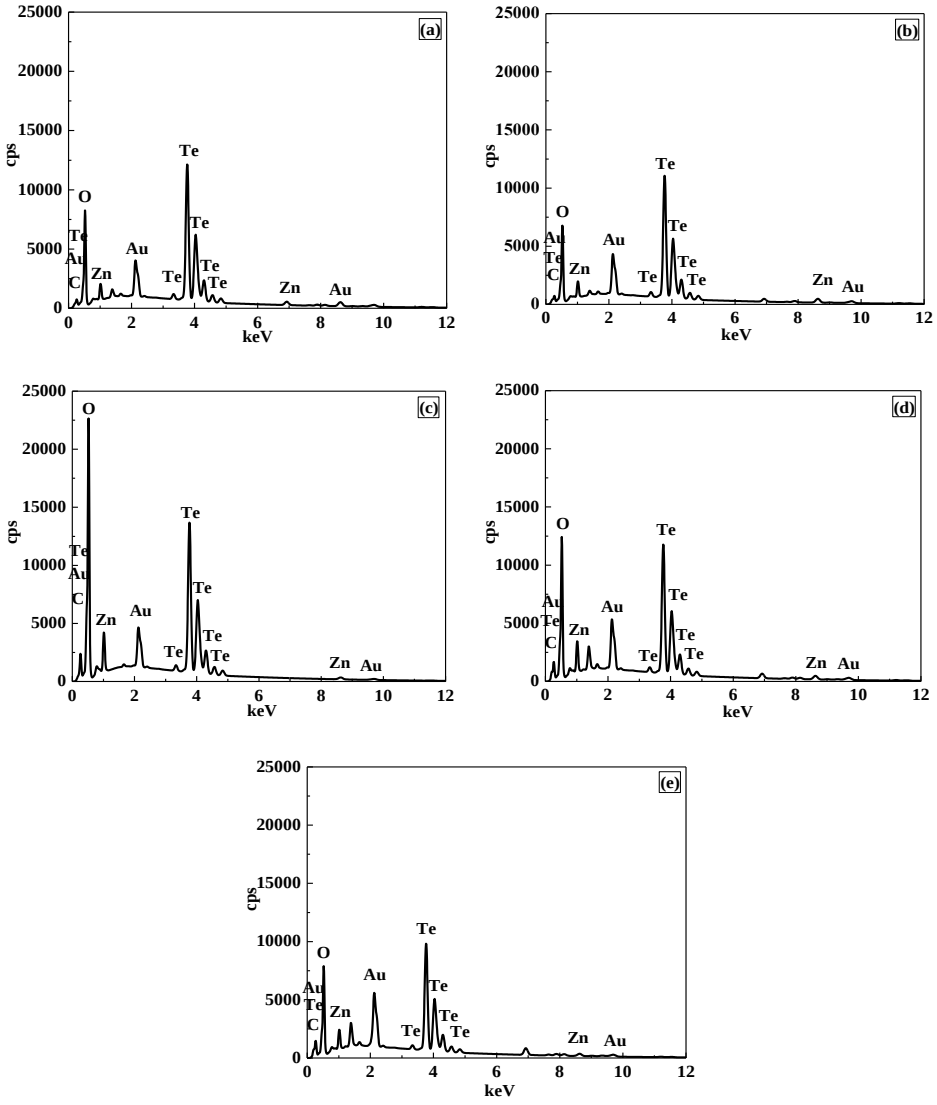

Fig. 8. EDX spectra of corroded glass with ammonium hydroxide as immersion solution for (a) TZNE glass (b) TZNE-HT325 glass (c) TZNE-HT350 glass (d) TZNE-HT375 glass and (e) TZNE-HT400 glass.

Tables 4 and 5 displayed variation in the elemental traces from EDX spectra of corroded glass by using distilled water and ammonium hydroxide as immersion solution. It can be observed that distilled water attacks glass former in the glass network which is reflected by the lower percentage of detected tellurium element as indicated in Table 4. In contrast, ammonium hydroxide solution attacks transition metal in the glass network which is reflected by the lower percentage of detected zinc element as indicated in Table 5. According to Paul [29], the formation of $HZnO_2^-$ and ZnO_2^{2-} ions from ZnO are likely to occur in alkaline environment. The activity of $HZnO_2^-$ and ZnO_2^{2-} ions are smaller than hydrated ZnO. Therefore, this feature makes glass containing zinc elements vulnerable to vigorous alkaline attack.

Table 4. Elemental traces from EDX spectra for glass immersed in distilled water.

Element	Series	Glass									
		TZNE		TZNE-HT325		TZNE-HT350		TZNE-HT375		TZNE-HT400	
		Weight (wt%)	Atomic (at%)	Weight (wt%)	Atomic (at%)	Weight (wt%)	Atomic (at%)	Weight (wt%)	Atomic (at%)	Weight (wt%)	Atomic (at%)
Carbon	K	0.61	3.35	4.37	19.12	0.79	4.23	0.96	5.07	0.97	4.74
Oxygen	K	9.54	39.58	12.74	41.87	10.43	41.87	10.73	42.66	13.25	48.47
Zinc	K	23.45	23.80	18.67	15.01	22.24	21.84	21.82	21.22	20.45	18.31
Tellurium	L	59.38	30.90	47.22	19.46	58.45	29.42	54.57	27.20	56.14	25.75
Gold	M	7.02	2.37	17.00	4.54	8.09	2.64	11.92	3.85	9.19	2.73
Total		100.00	100.00	100.00	100.00	100.00	100.00	100.00	100.00	100.00	100.00

Table 5. Elemental traces from EDX spectra for glass immersed in ammonium hydroxide solution.

Element	Series	Glass									
		TZNE		TZNE-HT325		TZNE-HT350		TZNE-HT375		TZNE-HT400	
		Weight (wt%)	Atomic (at%)	Weight (wt%)	Atomic (at%)	Weight (wt%)	Atomic (at%)	Weight (wt%)	Atomic (at%)	Weight (wt%)	Atomic (at%)
Carbon	K	0.78	4.13	4.89	27.82	0.55	3.13	1.35	7.10	0.71	3.79
Oxygen	K	13.11	52.43	-	-	11.88	50.05	12.47	49.11	12.36	49.24
Zinc	K	4.38	4.29	8.68	12.09	6.07	6.26	9.44	9.09	8.83	8.61
Tellurium	L	71.23	35.74	79.96	57.09	68.06	35.96	58.41	28.84	74.37	37.15
Gold	M	10.50	3.41	6.47	3.00	13.44	4.60	18.33	5.86	3.73	1.21
Total		100.00	100.00	100.00	100.00	100.00	100.00	100.00	100.00	100.00	100.00

4. Conclusion

This study demonstrated the variation in thermal stability, chemical durability, and surface morphology of tellurite glass by varying the heat treatment temperature. The aforementioned features of the studied glass were found to depend strongly on the heat treatment due to the generation of NBO. The thermal stability of TZNE glass higher than 100 °C reflects good thermal stability. The highest weight loss percentage of glass was observed in ammonium hydroxide solution (64.55−102.28%) compared to the distilled water (3.88−40.26%), which was due to the vigorous attack of hydroxyl ion from the ammonium hydroxide solution to the glass network. The SEM images displayed the emergence of different shapes and sizes of particles deposited on the glass surface due to chemical reactions that occurred between the glass and aqueous solution. The careful tuning of specific parameters and significant findings of the current study may contribute to the development of potential glass for intense weathering conditions.

Acknowledgements

The authors are thankful to Ministry of Higher Education Malaysia (MoHE) and Universiti Malaysia Sabah (UMS) for the financial support under Fundamental Research Grant Scheme (vote FRG0507-1/2019), Innovation Grant Scheme (vote SGI0053-2018) and UMSGreat Grant Scheme (GUG0325-1/2019).

References

[1] N. Papadopoulos, C. A. Drosou, J. Univ. Chem. Technol. Metallurgy **47**, 429 (2012).
[2] Z. A. El-Hadi, Chem. Papers **49**, 16 (1995).
[3] R. G. Newton, Glass Technology **26**, 21 (1985).

[4] R. de Almeida, D. M. da Silva, L. R. P. Kassab, C. B. de Araujo, Opt. Commun. **281**, 108 (2008).
[5] S. P. A. Osorio, V. A. G. Rivera, L. A. O. Nunes, E. Marega Jr., D. Manzani, Y. Messaddeq, Plasmonics **7**, 53 (2012).
[6] M. R. Dousti, M. R. Sahar, S. K. Ghoshal, R. J. Amjad, R. Arifin, J. Non-Cryst. Solids **358**, 2939 (2012).
[7] B. J. Riley, J. O. Kroll, J. A. Peterson, D. A. Pierce, W. L. Ebert, B. D. Williams, M. M. V. Snyder, S. M. Frank, J. L. George, K. Kruska, J. Nuclear Mat. **495**, 405 (2017).
[8] Z. A. S. Mahraz, M. R. Sahar, S. K. Ghoshal, Chalcogenide Lett. **11**, 453 (2014).
[9] B-H. Kim, B-A. Kang, Y-H. Yun, K-S. Hwang, Mat. Sci-Pol. **22**, 83 (2004).
[10] W. Ahmina, M. E. Moudane, M. Zriouil, M. Cherraj, M. Taibi, MATEC Web Conf. **149**, 01081 (2018).
[13] S. T. Bashir, L. Yang, J. J. Liggat, J. L. Thomason, J. Mater. Sci. **53**, 1710 (2018).
[14] M. R. Dousti, P. Ghassemi, M. R. Sahar, Z. A. Mahraz, Chalcogenide Lett. **11**, 111 (2014).
[11] M. Walas, T. Lewandowski, A. Synak, M. Lapinski, W. Sadowski, B. Koscielska, J. Alloys Compd. **696**, 619 (2017).
[12] F. A. Santos, J. R. J. Delben, A. A. S. T. Delben, L. H. C. Andrade, S. M. Lima, J. Non-Cryst. Solids **357**, 2907 (2011).
[15] L. Heireche, M. M. Heireche, M. Belhadji, J. Non-Oxide Glasses **10**, 83 (2018).
[16] Deepika, K. S. Rathore, N. S. Saxena, Appl. Phys. A **98**, 441 (2010).
[17] I. Jlassi, H. Elhouichet, S. Hraiech, M. Ferid, J. Lumin. **132**, 832 (2013).
[18] M. Reben, J. Wasylak, B. Burtan, J. Jaglarz, J. Cisowski, B. Jarzabek, M. Lisiecki, Proc. of SPIE. **8010**, 80100L-1 (2011).
[19] P. Babu, H. J. Seo, C. R. Kesavulu, K. H. Jang, C. K. Javasankar, J. Lumin. **129**, 444 (2009).
[20] L. Cormier, Proc. Mat. Sci. **7**, 60 (2014).
[21] A. Nukui, S-I. Todoroki, M. Miyata, Y. Bando, Mat. Trans. **43**, 355 (2002).
[22] M. Dolhen, M. Tanaka, V. Couderc, S. Chenu, G. Delaizir, T. Hayakawa, J. Cornette, F. Brisset, M. Colas, P. Thomas, J-R. Duclere, Sci. Rep. **8**, 4640 (2018).
[23] H. A. Elbatal, M. A. Azooz, E. A. Saad, F. M. EzzELDin, M. S. Amin, Silicon **10**, 1139 (2018).
[24] I. C. Popovici, N. Lupascu, Ovidius Univ. Annals Chem. **23**, 128 (2012).
[25] G. P. Singh, P. Kaur, S. Kaur, D. P. Singh, Physica B **407**, 4168 (2012).
[26] H. V. Walters, P. B. Adams, Appl. Opt. **7**, 845 (1968).
[27] J. F. Stebbins, E. V. Dubinsky, K. Kanehashi, K. E. Kelsey, Geochim. et Cosmochim. Acta **27**, 910 (2008).
[28] J-Y. Pyo, C. W. Lee, H-S. Park, J. H. Yang, W. U. J. Heo, J. Nuclear Mat. **493**, 1 (2017).
[29] A. Paul, Chapman and Hall, London. 1982.
[30] S. K. Ghoshal, A. Awang, M. R. Sahar, R. Arifin, J. Lumin. **159**, 265 (2015).